Immobilization of calcium phosphate nano-clusters into alkoxy-derived porous TiO_2 coatings

M. SHIRKHANZADEH, S. SIMS
Department of Materials and Metallurgical Engineering, Queen's University, Kingston, Ontario, Canada K7L 3N6

Alkoxy-derived porous coatings of titanium oxide were fabricated on commercially pure titanium substrates by an electrochemical method in methanolic electrolytes. Nano-clusters of brushite ($CaHPO_4 \cdot 2H_2O$) were immobilized into the pores of the oxide network by reacting these coatings in acidic calcium phosphate solutions at 50 °C. The acid-base reaction between calcium phosphate solutions and the hydroxyl groups of the oxide network resulted in the formation of nano-clusters of brushite crystals immobilized inside the oxide pores. This treatment resulted in the conversion of the porous oxide network into a coherent mass with improved physical integrity. Nano-clusters of brushite crystals immobilized in the oxide matrix were converted into amorphous calcium phosphate (ACP) and poorly crystallized hydroxyapatite (HA) by further treatment of the oxide in alkaline solutions. The porous oxide coating also reacted strongly with concentrated phosphoric acid. The phosphate-modified oxide resulting from this reaction was further treated in calcium hydroxide solution to form nano-clusters of poorly crystallized HA within the oxide network.

1. Introduction

Titanium is known to be biocompatible and has shown impressive clinical results as a dental and orthopaedic implant material. Light microscopic and ultrastructural analyses have revealed evidence of osseointegration, a direct bone-to-implant contact [1]. The excellent tissue response to titanium is believed to be related to the chemical and biochemical properties of titanium oxide at the titanium surface [2]. Auger electron spectroscopy (AES) studies on titanium implants retrieved from bone have shown a large increase in the oxide thickness and incorporation of calcium and phosphates into the oxide after a long implantation time [3]. The incorporation of calcium and phosphates into the oxide may be a crucial step in the bone-bonding process. Properties of the oxide, such as chemical composition, stoichiometry, defect density, crystal structure and porosity, may determine the diffusion rate of calcium and phosphate ions into the oxide and the rate of the bone-bonding process. We have previously reported an electrochemical process for the fabrication of alkoxy-derived titanium oxide coatings (up to 40 μm thick) at room temperature [4–6]. The process involves direct synthesis of titanium methoxide ($Ti(OCH_3)_4$) by anodic oxidation of titanium in methanolic electrolytes and its rapid hydrolysis and conversion into titanium oxide in the presence of water. In this process, an inorganic network consisting of Ti–O–Ti bridges is formed on the titanium substrate as a result of hydrolysis and controlled polycondensation of titanium methoxide. The polycondensed oxide network formed on the Ti substrate is nano-porous and poorly crystallized at room temperature and contains numerous OH groups [4]. It is envisaged that such a porous oxide network may facilitate fast diffusion of calcium and phosphorous ions, and may allow calcium phosphate nano-clusters to be synthesized within the nanometre-sized pores in the oxide matrix at suitable pH values. Thus biocompatible coatings with novel combinations of properties may be synthesized.

The objective of this research was to investigate the possibility of incorporating nano-clusters of brushite and poorly crystalline hydroxyapatite into the alkoxy-derived coatings.

2. Materials and methods

Nano-clusters of brushite ($CaHPO_4 \cdot 2H_2O$) were immobilized into alkoxy-derived porous titanium oxide coatings by reacting these coatings in 0.2 M brushite solutions (pH = 2.7) at 50 °C for various time intervals up to 24 h. These coatings were subsequently treated in 0.1 M $Ca(OH)_2$ and NaOH solutions to convert the brushite into amorphous calcium phosphate (ACP) and poorly crystallized hydroxyapatite (HA), respectively. Alkoxy-derived coatings (12 μm thick) were fabricated on commercially pure titanium plates ($3 \times 5\ cm^2$) which were etched in hydrofluoric acid (HF). The oxide coatings were prepared at constant voltage (5 V) for 1 h in methanolic electrolytes

0957–4530

according to the procedures described earlier [6]. The electrolyte was made by adding 10 g analytical reagent sodium nitrate ($NaNO_3$) to 1 l of analytical reagent methanol containing less than 1% water. The microstructure of the oxide coating was determined by X-ray diffraction (XRD) technique using CoK_α radiation. X-ray diffractions were obtained using the glancing angle technique at an angle of incidence of 5°. A Rigaku 12 KW rotating anode generator was used, equipped with a D Max diffractometer with a thin film attachment. X-ray photoelectron spectroscopy (XPS) was also employed to identify the physisorbed and chemisorbed hydroxyls on the oxide surface. Simultaneous thermogravimetric and differential thermal analysis (TG and DTA) were carried out using 25 mg of the oxide powder at a heating rate of 10 °C min^{-1} in air to gain further information with regard to the structure of the oxide coating.

Fourier transformed infrared (FTIR) spectroscopy was used to investigate the nature of the interactions between the oxide coating and the acidic brushite solutions and to characterize the calcium phosphate phases immobilized within the porous oxide network. Scanning electron microscopy (SEM) and thin-film X-ray diffraction techniques were also employed to examine the surface morphology and the crystal structure of reaction products formed on the oxide surface.

3. Results and discussion

3.1. Characterization of the alkoxy-derived coating

Extensive characterization of the alkoxy-derived oxide coating has been published previously [4–6]. In what follows we summarize those characteristics which are essential for the analysis of the results in the present work. As shown in Fig. 1, thin film X-ray diffraction of the as-prepared oxide coating exhibited a broad peak over a range of 2 θ values between 30 to 50, indicating that the oxide coating is poorly crystallized at room temperature and may consist of ultrafine crystallites. It should be noted that in almost all cases, alkoxy-derived (sol–gel) titania is either amorphous or poorly crystallized in the anatase form [7]. Previous work [6] has indicated that the post treatment of the oxide coating results in the formation of a well-defined nano-crystalline anatase phase with a grain size ranging from 5 nm at 400 °C to 30 nm at 800 °C. The simultaneous TG and DTA curves of the oxide are shown in Fig. 2. The TG curve shows three stages of mass loss. Stage 1, *c.* 20–150 °C, shows a mass loss of *c.* 10% and is accompanied by a large endotherm and can be attributed to the loss of loosely bound water (i.e. physisorbed water) present within the pores of the oxide. Stage 2, *c.* 150–270 °C, involves a gradual mass loss. It is likely that any carbonaceous residue in the oxide network may be lost at this stage. Stage 3 is characterized by an initial rapid loss of mass at about 300 °C followed by a gradual mass loss. The endotherm associated with the mass loss at this stage interrupts the exotherm assigned to crystallization. The rapid loss of mass in Stage 3 may be due to the loss of strongly bound water (i.e. chemisorbed water). Further evidence for the presence of physisorbed and chemisorbed water in the oxide network comes from the high resolution XPS O1s spectrum (Fig. 3). The major peak at 530.5 eV was attributed to bulk oxygen of the oxide and the subpeaks at 531.7 and 533.2 eV were assigned to physisorption of (OH) and chemisorbed H_2O (i.e. Ti–OH), respectively. These results indicate that as-prepared coatings may consist

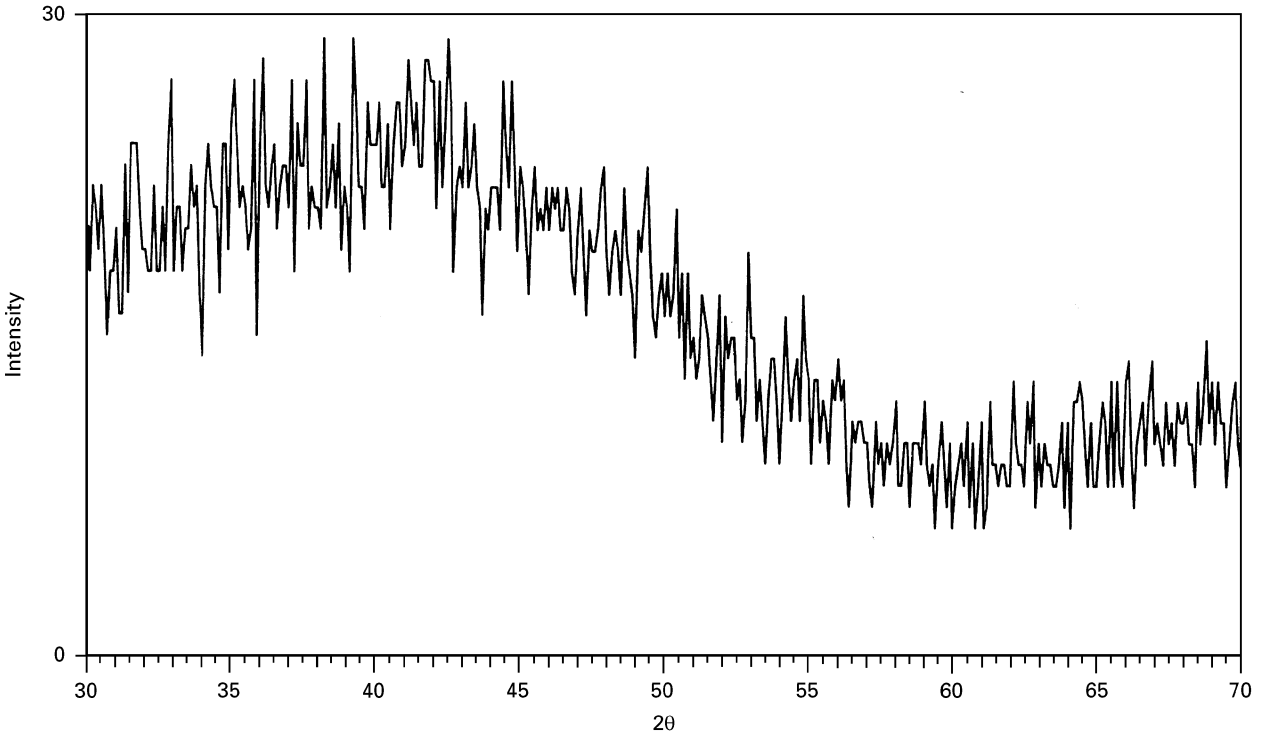

Figure 1 Thin-film X-ray diffraction pattern of the as-prepared alkoxy-derived TiO_2 coating.

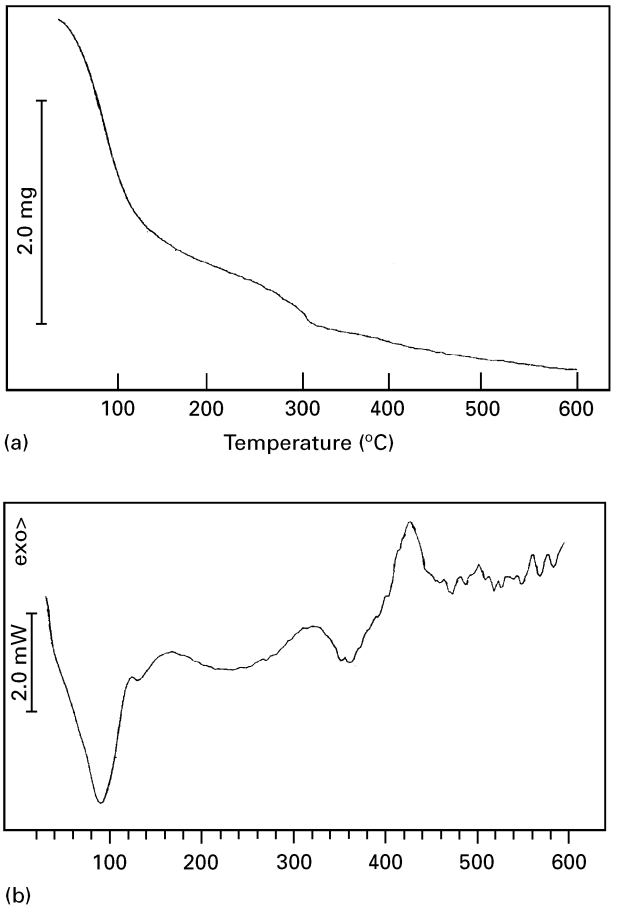

Figure 2 Simultaneous (a) TG and (b) DTA of the alkoxy-derived TiO_2 coating.

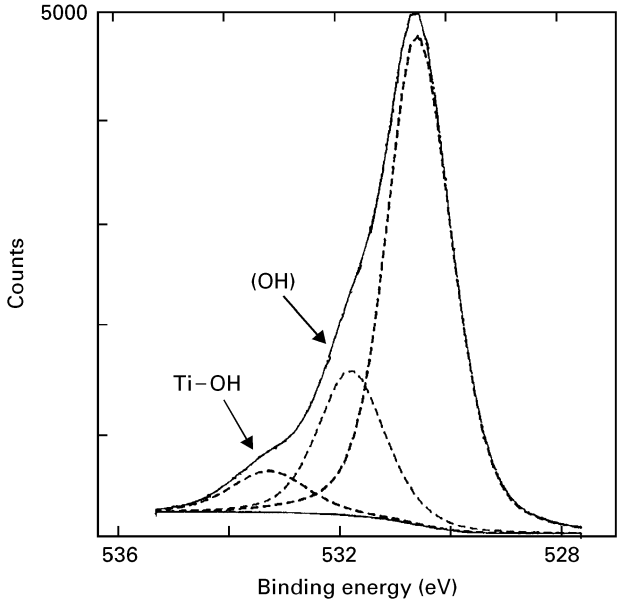

Figure 3 High resolution XPS spectrum of the $O1_s$ peak at the oxide surface.

of a hydrated oxide network, containing nanometre-sized pores occupied by loosely bound water similar to xerogels of titania prepared by the sol–gel method [8]. The xerogel films prepared by the sol–gel method, however, are normally thin and need heating in order to obtain a stable film, during which the occupied pores may collapse, leading to considerable shrinkage of the material. The as-prepared oxide network synthesized by the electrochemical method, on the other hand, is stable at room temperature and it is well-adhered to the substrate without heat treatment. Density measurement has shown that these coatings maintain their porous structure even after heat treatment and attain only 70% of the theoretical density of the fully dense TiO_2 when heated to 400 °C.

3.2. Formation of nano-clusters of brushite within the oxide matrix

Fig. 4 shows the FTIR spectra of the titanium oxide coating incubated in the acidic brushite solution at 50 °C for various time periods. For comparison, the FTIR spectrum of the bulk brushite is also presented in this figure. From Fig. 4, it is seen that the alkoxy-derived oxide acts as an efficient substrate for the nucleation and growth of brushite in acidic solutions. The IR bands associated with the P–O

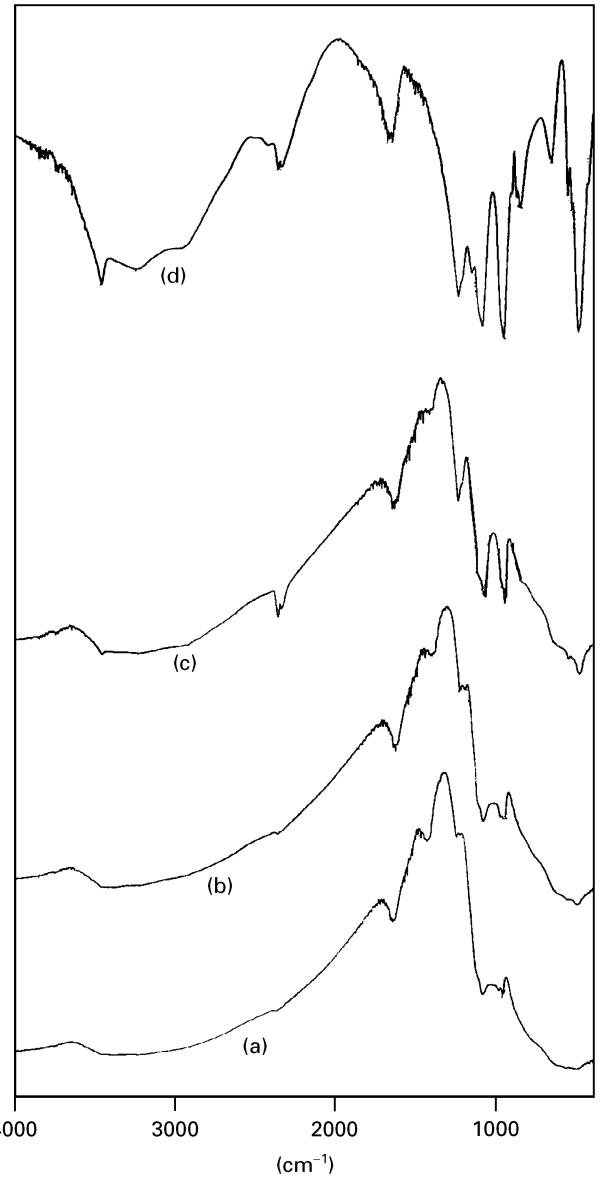

Figure 4 FTIR spectra of the titanium oxide coating incubated in the acidic brushite solution at 50 °C for (a) 10 min; (b) 30 min; and (c) 60 min. FTIR of the bulk brushite (d) is shown for comparison.

bonds of brushite are evident in the oxide spectrum even after 10 min treatment. Similar results were also obtained at room temperature but after a relatively longer time (Fig. 5). As seen in Fig. 5, heat treatment of the oxide coating at 300 °C for only 20 min significantly reduced the extent of the interaction between the oxide and the acidic brushite solution. The reduced rate of the reaction may be due to the loss of hydroxyls of the oxide as evident from the TG and DTA results (Fig. 2). It is also known that alkoxy-derived oxides may undergo densification at high temperatures. Therefore, the diffusion rate of reacting ions (e.g. $H_2PO_4^-$) through pores of the oxide may be significantly limited. The results in Fig. 5 further demonstrate that a suitable substrate such as hydrated titania is essential for the nucleation and growth of brushite under the present experimental conditions. Nucleation of brushite may be facilitated by the chemical interaction between the hydrated oxide and the phosphate ions present in the solution. It is known that the surface hydroxyl groups of titania in solutions tend to be polarized and electrically charged [9]. The hydroxyls of titania are protonated and positively charged below its isoelectric point (IEP) of pH 6.2.

$$\text{Ti–OH} + \text{H}^+ \rightarrow \text{Ti–OH}_2^+ \qquad (1)$$

At acidic pH values less than 6.2, $H_2PO_4^-$ species can be adsorbed on the positively charged titania surface. The adsorption of $H_2PO_4^-$ anion on titania may involve an exchange reaction between surface hydroxyl groups and the $H_2PO_4^-$ species as suggested by Flaig-Baumann *et al.* [10]. The interaction can be presented as

$$\begin{aligned} &\text{O–Ti–OH} + \text{H}^+ + \text{H}_2\text{PO}_4^- \\ &= \text{O–Ti–OH}_2 = \text{O–Ti–PO}_4\text{H}_2 + \text{H}_2\text{O} \qquad (2) \\ &\quad\ \ | \\ &\quad\ \ \text{PO}_4\text{H}_2 \end{aligned}$$

Formation of brushite may be initiated once the surface concentration of the phosphate species is sufficiently high and the supersaturation exceeds the level necessary for the heterogenous nucleation of brushite.

SEM was used to examine the surface morphology of the oxide treated in brushite solutions. An extremely thin film of brushite was evident on the oxide surface after 60 min treatment in acidic brushite solutions (Fig. 6).

SEM examination of the oxide treated for shorter times did not show evidence of brushite on the oxide surface. Despite this, intense IR bands associated with the acid phosphate groups of brushite were observed in the IR spectra of the powdered oxide (Fig. 4) even after 10 min treatment, indicating that a considerable amount of brushite was indeed trapped within the porous oxide network. As seen in Fig. 4, the positions of the absorption bands associated with the brushite phase formed in the oxide pores at early stages do not coincide with those of the bulk brushite. The shift of the IR bands can be interpreted in terms of formation of a chemical bond between initially deposited brushite phase and the porous oxide matrix. The formation of this bond will result in distortion of the equilibrium atomic positions of the phosphate groups in brushite. Such changes in the structural milieu surrounding these ions may in turn result in the band shift to the lower frequencies. Another significant observation supporting the formation of this chemical bond was that coatings treated in acidic brushite solutions for short times were considerably more difficult to scrape off from the substrate than the untreated coatings. The formation of a chemical bond between brushite and the oxide apparently results in

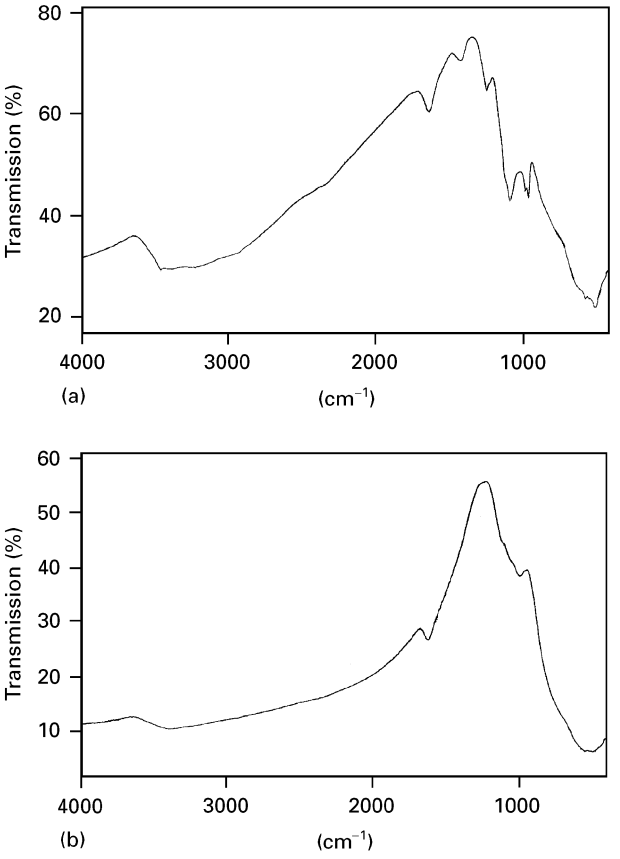

Figure 5 FTIR spectra of the titanium oxide coating incubated in the acidic brushite solution at room temperature for 24 h: (a) as-prepared oxide; (b) oxide coating heat treated at 300 °C for 20 min.

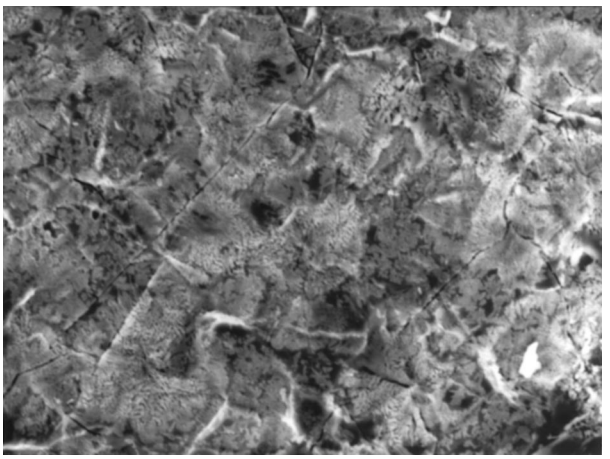

Figure 6 SEM micrograph of the oxide surface after incubation in acidic brushite solution at 50 °C for 60 min (× 800).

the conversion of the porous oxide matrix into a more coherent mass with improved integrity.

3.3. Formation of nano-clusters of poorly crystallized hydroxyapatite in the oxide matrix

It was of interest to see if brushite entrapped in the oxide matrix can be converted to a basic calcium phosphate phase. For this purpose, oxide coatings impregnated with brushite for 60 min were further treated in 0.1 M $Ca(OH)_2$ solutions at 85 °C for 75 min. No deposit was detected on the oxide surface after this treatment. Apparently, fine crystals of brushite present on the oxide surface were easily washed away from the surface during treatment in $Ca(OH)_2$ solution. FTIR of the powdered oxide removed from the substrate (Fig. 7), however, indicated that brushite entrapped in the oxide matrix was substantially converted to amorphous calcium phosphate (ACP). The broad featureless absorbance bands in the 500–700 cm^{-1} and 1035 cm^{-1} observed in Fig. 7 are the main characteristics of ACP [11–13]. These bands arise primarily from the anti-symmetric P–O stretching (ν3) and bending (ν4) modes of the ACP phosphate groups. The presence of a spectral feature at 1422 cm^{-1} arising in part from a carbonate asymmetric stretching mode [14] suggests that carbonate substitution has also taken place. No IR bands associated with the crystalline hydroxyapatite are detected in Fig. 7. The conversion of brushite to ACP rather than to HA is not surprising. Boskey and Posner [15] have shown that in the presence of high concentrations of calcium and phosphate (each greater than 10 mM) and at pH values greater than 6.8, the precipitation of hydroxyapatite is always preceded by the spontaneous formation of an amorphous phase. The conversion of the amorphous phase to HA is shown to be an autocatalytic process with the rate of conversion dependent on the pH and the ionic strength of the mediating solution. The rate of autocatalytic conversion of the ACP to hydroxyapatite in alkaline solutions is reported to be slow [15]. Thus a relatively long term treatment would be required to completely convert ACP to hydroxyapatite. FTIR spectrum of

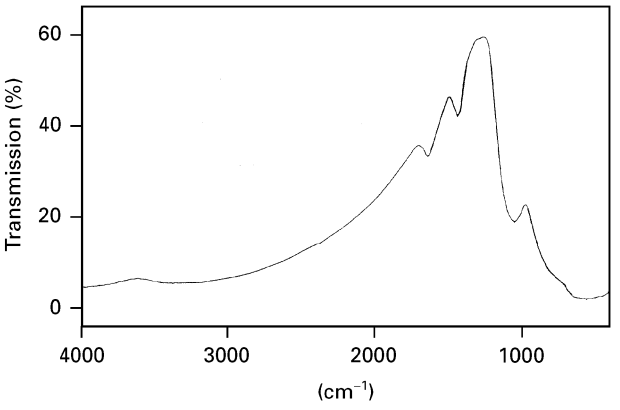

Figure 7 FTIR spectrum of the burshite-impregnated oxide after treatment in 0.1 M Ca(OH) at 85 °C for 75 min.

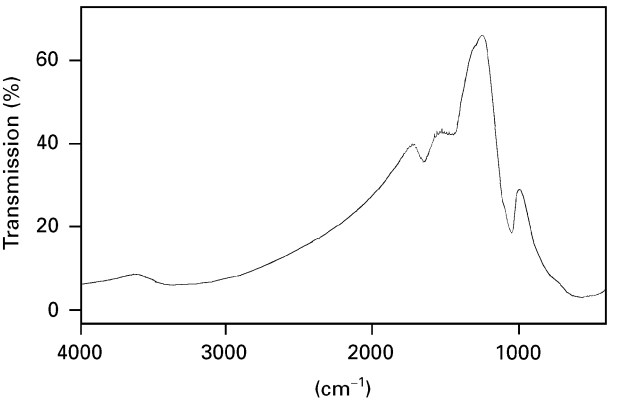

Figure 8 FTIR spectrum of the brushite-impregnated oxide after treatment in 0.1 M NaOH at 85 °C for 24 h.

the brushite-impregnated oxide after an extended treatment (24 h) in 0.1 M NaOH at 50 °C is shown in Fig. 8. Close examination of this spectrum shows that qualitatively the shape of the ν3 P–O absorbance has changed from the broad, featureless profile observed for the ACP to a composite of overlapping narrow bands from which a high frequency shoulder at 1090 cm^{-1} emerges. The narrow band at 1040 cm^{-1} and the weak shoulder at 1090 cm^{-1} are the main components of ν3 absorbance of poorly crystalline hydroxyapatite in a matrix of ACP. Such spectral changes have also been observed by Stutman and co-workers [11] and Pleshko *et al.* [12] during the solution-mediated transformation of ACP to poorly crystalline hydroxyapatite. The spectral features at 1040 and 1090 cm^{-1} are also similar to those observed in the IR spectrum of poorly crystalline bone minerals [12]. Eanes and Meyer [16] have shown that crystals grown by conversion of ACP in solutions are not shape-stable. Marked changes in the size and the relative proportion between crystal dimensions takes place with ageing. These alterations indicate an underlying phase change or a change in the atomic configuration and/or composition on one set of growing faces. Similar alterations in crystal size and shape may also occur during the conversion of ACP to poorly crystallized hydroxyapatite in the porous oxide network. However, these changes may be severely limited due to the relative rigidity of the oxide network. It is interesting to note that the growth and maturation of poorly crystalline hydroxyapatite in the organic matrix of newly synthesized bone is also limited by the small geometry of the hole zones of the collagen fibrils [17].

Poorly crystallized hydroxyapatite was also incorporated into the oxide network by first treating the oxide in concentrated phosphoric acid for 24 h to form a phosphate-modified oxide network and then reacting this modified oxide with 0.1 M $Ca(OH)_2$ to form poorly crystallized hydroxyapatite. The phosphate-modified oxide network reacted strongly with $Ca(OH)_2$ solution. The FTIR spectrum of the oxide coating removed from the substrate after this treatment (Fig. 9) indicated that the reaction product was substantially poorly crystallized hydroxyapatite. This was also confirmed by thin film X-ray diffraction

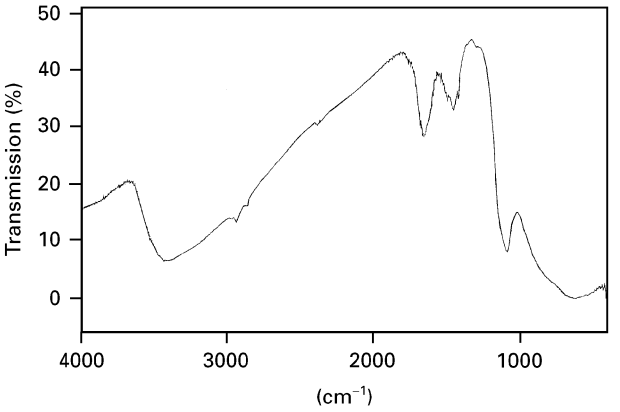

Figure 9 FTIR spectrum of the phosphate-modified oxide after treatment in 0.1 M Ca(OH) at 85 °C for 8 h.

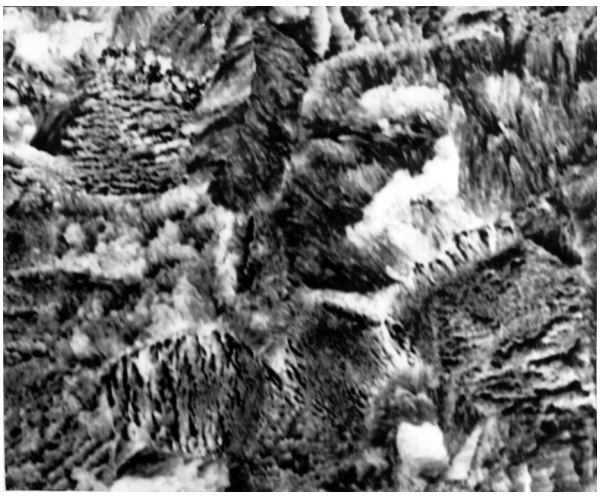

Figure 11 Surface morphology of the poorly crystallized hydroxyapatite formed on the phosphate-modified oxide after incubation of the oxide in 0.1 M Ca(OH) at 85°C for 8 h (×1560).

analysis (Fig. 10). As is evident from Fig. 11, a substantial amount of poorly crystalline hydroxyapatite is formed on the oxide surface as a result of the interaction between phosphate groups in the oxide and Ca ions in the solution. This clearly demonstrates that phosphate groups are not exclusively located on the surface and that a large amount of phosphate groups are indeed incorporated within the porous oxide network during phosphoric acid treatment. Although the exact concentration of adsorbed phosphate groups within the oxide network is unknown, it has been suggested that ~ 1.6 $H_2PO_4^-$ groups/nm^2 exist on anatase and rutile surfaces [18]. The porous oxide network apparently not only facilitates fast diffusion of phosphate ions but also provides a large surface area which is required for the effective adsorption of these species. It is speculated that during calcium hydroxide treatment, phosphate species are exchanged with hydroxyl ions and liberated as orthophosphate ions:

$$\text{O–Ti–PO}_4\text{H}_2 + 3\text{OH}^- \rightarrow \text{PO}_4^{3-} + 2\text{H}_2\text{O} + \text{O–Ti–OH} \quad (3)$$

Once liberated, phosphate ions can readily react with Ca ions to form poorly crystallized hydroxyapatite. However, calcium ions with an ionic radius of 0.099 nm [19] would be expected to infiltrate the porous oxide faster than phosphate ions (ionic radius of 0.4–0.6 nm [20]) can diffuse out. Thus, although it appears that poorly crystallized hydroxyapatite nucleate first on the oxide surface, the mobility of phosphate ions in the pores is considerably lower than

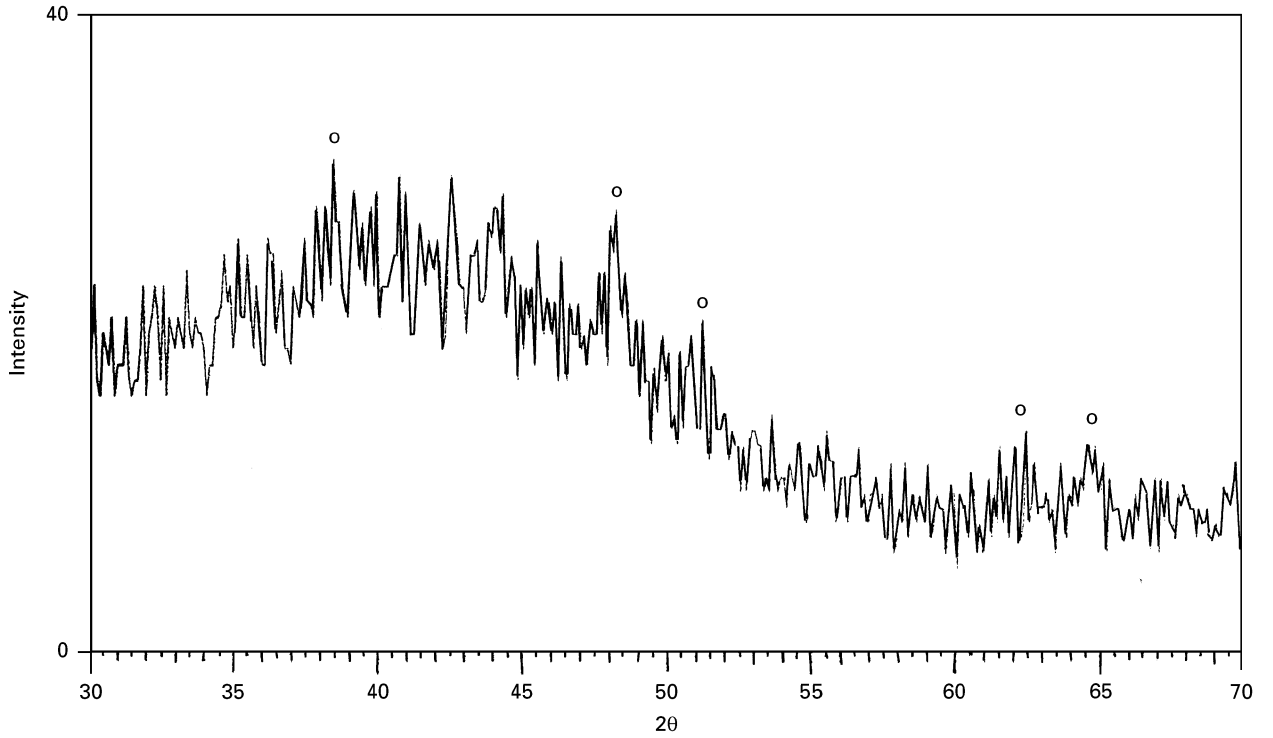

Figure 10 Thin-film X-ray diffraction of the reaction product formed on the phosphate-modified oxide after treatment in 0.1 M Ca(OH) at 85 °C for 8 h (o apatite).

Ca ions, implying that calcium infiltrates throughout the depth of the porous oxide to form poorly crystallized hydroxyapatite.

Work in progress shows that nano-porous TiO_2 coating is also an effective substrate for immobilization of organic compounds such as amino acids, peptides and proteins. Proteins of high molecular weight, and particularly phosphoproteins, are strongly retained by nano-porous TiO_2 coatings, presumably by the multi-attachment of their polar groups to the porous oxide matrix.

4. Conclusions

The results in this work have shown that nano-clusters of brushite, ACP and poorly crystallized hydroxyapatite can be incorporated into nano-porous alkoxy-derived oxide coatings at suitable pH values. The formation of a chemical bond between calcium phosphate clusters and the oxide results in the conversion of the porous oxide matrix into a coherent mass with improved integrity. The apparent ability of Ca and phosphate ions to permeate the alkoxy-derived oxide network in short times calls into question the possibility of the formation of similar chemical bonds *in vivo*. Animal implantation studies are required to investigate this possibility and to assess the potential use of these coatings for accelerating the process of osseointegration *in vivo*.

Acknowledgements

The authors thank the Natural Sciences and Engineering Research Council of Canada (NSERC) for the financial support provided for this research project.

References

1. C. JOHNSSON and T. ALBREKTSSON, *J. Oral Maxillo Fac. Implants* **2** (1987) 69.
2. B. KASEMO, *J. Prosthet. Dent.* **49** (1989) 832.
3. J. E. SUNDGREN, P. BODÖ and I. LUNDSTRÖM, *J. Colloid Interface. Sci.* **110** (1986) 9.
4. M. SHIRKHANZADEH, *J. Mater. Sci. Mater. Med.* **6** (1995) 206.
5. *Idem*, *ibid.* **3** (1992) 322.
6. *Idem*, *Nanostructured Mater.* **5** (1995) 33.
7. C. J. BRINKER and G. W. SCHERER, "Sol-Gel Science" (Academic Press, London, 1990).
8. A. DAVIES, R. J. HOBSON, M. J. HUDSON, W. J. MACLIN and R. J. NEAT, *J. Mater. Chem.* **6** (1996) 49.
9. G. A. PARKS, *Chem. Rev.* **65** (1965) 177.
10. R. FLAIG-BAUMANN, M. HERMANN and H. P. BOEHM, *Z. Anorg. Allg. Chem.* **372** (1970) 296.
11. J. M. STUTMAN, J. D. TERMINE and A. S. POSNER, *Trans. New York Acad. Sci.* **29** (1966) 669.
12. N. PLESHKO, R. BOSKEY and R. MENDELSOHN, *Biophys. J.* **60** (1991) 786.
13. R. MENDELSOHN, A. HASSANKHANI, E. DICARLO and A. BOSKEY, *Calcif. Tissue Int.* **44** (1989) 20.
14. M. VIGNOLES, G. BONEL, D. W. HOLCOMB and R. A. YOUNG, *ibid.* **43** (1988) 33.
15. A. L. BOSKEY and A. S. POSNER, *J. Phys. Chem.* **77** (1973) 2313.
16. E. D. EANES and J. L. MEYER, *Calcif. Tissue Res.* **23** (1977) 259.
17. H. M. KIM, C. REY and M. J. GLIMCHER, *J. Bone Miner. Res.* **10** (1995) 1589.
18. General Discussion, *Disc. Faraday Soc.* **52** (1971) 276.
19. R. D. SHANON and C. T. PREWITT, *Acta Crystallogr.* **25** (1969) 925.
20. M. M. PEREIRA, A. E. CLARK and L. L. HENCH, *J. Amer. Ceram. Soc.* **78** (1995) 2463.

Received 16 October
and accepted 19 November 1996